International Journal of Biochemistry and Cell Biology 107 (2019) 53–61

Contents lists available at ScienceDirect

International Journal of Biochemistry and Cell Biology

journal homepage: www.elsevier.com/locate/biocel

Mass spectrometry-based peptidome profiling of human serous ovarian cancer tissues

Juan Xu[a,1], Xusu Wang[a,1], Pengfei Xu[b,1], Siyu Liu[a], Fang Teng[a], Xiaoguang Liu[a], Qiaoying Zhu[a], Xiangdong Hua[a], Zhen Gong[a], Xuemei Jia[a,*]

[a] Department of Obstetrics and Gynecology, Women's Hospital of Nanjing Medical University (Nanjing Maternity and Child Health Care Hospital), Nanjing, 210004, China
[b] Nanjing Maternal and Child Health Institute, Women's Hospital of Nanjing Medical University (Nanjing Maternity and Child Health Care Hospital), Nanjing, 210004, China

ARTICLE INFO

Keywords:
Ovarian cancer
Endogenous peptides
Liquid Chromatography/Mass spectrometry
Cleavage sites
P1 derived from S38AA protein

ABSTRACT

Background: Bioactive peptides existing in vivo have been considered as an important class of natural medicines for the treatment of diseases. Peptidome analysis of tissues and biofluids had provided important information about the differentially expressed bioactive peptides in vivo.

Methods: Here, we analyzed the peptidome of serous ovarian cancer tissue samples and normal ovarian epithelial tissue samples by mass spectrometry and further investigated the possible bioactive peptides that were differentially expressed.

Results: We identified 634 differentially expressed peptides, 508 of these peptides were highly abundant in serous ovarian cancer tissues, a result consistent with higher protease activity in ovarian cancer patients. The difference in preferred cleavage sites between the serous ovarian cancer tissues and normal ovarian epithelium indicated the characteristic peptidome of ovarian cancer and the nature of cancer-associated protease activity. Interestingly, KEGG pathway analysis of the peptide precursors indicated that the differentially regulated pathways in ovarian cancer are highly consistent with the pathways discovered in other cancers. Besides, we found that a proportion of the differentially expressed peptides are similar to the known immune-regulatory peptides and anti-bacterial peptides. Then we further investigated the function of the two down-regulated peptides in ovarian cancer cells and found that peptide P1DS significantly inhibited the invasion and migration of OVCAR3 and SKOV3 ovarian cancer cells.

Conclusions: Our results are the first to identify the differentially expressed peptides between the serous ovarian cancer tissue and the normal ovarian epithelium. Our results indicate that bioactive peptides involved in tumorigenesis are existed in vivo.

1. Introduction

Ovarian cancer is the fifth leading cause of gynecological cancer deaths. Ovarian cancer is typically clinically silent in the early stages of disease. Surgery and chemotherapy with paclitaxel and platinum are the most common treatments worldwide. However, many ovarian cancer patients display only a transient response to the chemotherapeutic drugs and eventually develop recurrent chemoresistant ovarian cancer (Wang et al., 2016). Furthermore, the toxicity caused by the chemotherapeutic drugs remains a clinical challenge. Development of new drugs, especially natural medicines, for the treatment of ovarian cancer is thus of great importance.

Therapeutic peptides, such as anticancer peptides and antibiotic peptides; as well as other peptides used to treat polycystic ovary syndrome (PCOS), diabetes and other diseases; have shown great potential and broad market prospects (Frøssing et al., 2017; Mann et al., 2017; Waghu et al., 2016; Gaborit et al., 2016). The number of new therapeutic peptides with higher specificity, lower immunogenicity and

Abbreviations: PCOS, polycystic ovary syndrome; KEGG, Kyoto encyclopedia of genes and genomes; GO, gene ontology; TMT, tandem mass tag; DAVID, databases for annotation, visualization and integrated discovery; PI, isoelectric point; MW, molecular weight; P1DS, peptide 1 derived from S38AA protein; P1DP, peptide 1 derived from PAPD7 protein; PCA, Principal Component Analysis

* Corresponding author at: Department of Obstetrics and Gynecology, Women's Hospital of Nanjing Medical University (Nanjing Maternity and Child Health Care Hospital), 123 Mochou Rd., Nanjing, 210004, China.
E-mail address: xmjia@njmu.edu.cn (X. Jia).
[1] These authors contributed equally to this work.

https://doi.org/10.1016/j.biocel.2018.12.004
Received 27 July 2018; Received in revised form 23 November 2018; Accepted 7 December 2018
Available online 11 December 2018
1357-2725/

higher safety continues to grow. Therapeutic peptides that are designed to mimic the functional domain of proteins, extracted from plants or animals, or screened using peptide libraries that are constructed from degraded protein fragments continue to be found and proven effective as cancer therapeutics. For example, the synthesized peptide targeting ErbB2 (Arpel et al., 2014), the peptide targeting mutant p53 (Soragni et al., 2016; Selivanova et al., 1997) and the prosaposin-derived therapeutic cyclic peptide targeting thrombospondin 1 (TSP-1) (Wang et al., 2016) were found to inhibit the malignant behavior of cancer by regulating processes such as cell proliferation, cell apoptosis and cell metastasis. More importantly, the drug-like cyclic peptide derived from prosaposin (PSAP) that targets TSP-1 in the tumor microenvironment can promote tumor regression in both the ID8 and the patient-derived tumor xenograft mouse models of ovarian cancer with no obvious side effects and no expectation of the development of drug resistance compared with the first-line drug treatment, cisplatin (Wang et al., 2016). These studies have presented a strong body of evidence supporting the great potential of peptide drugs for the treatment of ovarian cancer.

Endogenous peptides, which are derived from endogenous proteolytic events or encoded by non-coding RNAs, are important regulators of biological processes (Lauressergues et al., 2015; Szafron et al., 2015; Matsumoto et al., 2017). Peptidome analysis can provide important information about proteolytic activity under relevant environmental conditions, as well as details about potential bioactive peptides. For example, the ectopic endometrial highly abundant peptide—PDFV promoted the migration and invasion of ESCs and reduced the expression of E-cadherin (Xue et al., 2018). In addition, a variety of functional peptides derived from milk have been found, including antimicrobial peptides, immunoregulatory peptides, and anti-arterial dysfunction peptides. Interestingly, the milk-derived fusion peptide ACFP, which showed immunoregulatory activity, also displayed tumor suppressor ability by promoting apoptosis in primary ovarian cancer (Zhou et al., 2016). These results further confirm the antitumor activity of peptides that exist in vivo.

Here, we carried out a quantitative liquid chromatography/mass spectrometry (LC/MS) analysis of human serous ovarian cancer tissue and normal ovarian epithelial tissue. The primary objectives were to establish the differences between the peptide profiles of normal ovarian epithelial tissue and serous ovarian cancer tissue and to identify potential antitumor peptides in vivo.

2. Materials and methods

2.1. Sample collection

All of the serous ovarian cancer tissue samples (n = 3; all samples were high grade and classified as FIGO stage IIIc in the histological analysis by the examining pathologists) and normal ovarian epithelium samples were collected from Women's Hospital of Nanjing Medical University (Nanjing Maternity and Child Health Care Hospital), Nanjing, China. All of the patients involved were postmenopausal and were age matched (58.33 ± 4.16 in the normal ovarian epithelial group and 62 ± 4.58 in the serous ovarian cancer group). The patients were informed about the research and signed medical informed consent documents, and this study was approved by the Ethical Committee of Women's Hospital of Nanjing Medical University (Nanjing Maternity and Child Health Care Hospital). And the methods were performed in accordance with the approved guidelines. All the tissues were collected immediately after surgery and were stored at −80°C until use.

2.2. Peptide extraction

The tissue samples were sectioned, crushed under liquid nitrogen, and then rapidly combined with 10 volumes of the extraction buffer containing protease inhibitor cocktail (Sigma-Aldrich, St. Louis, MO) and 0.25% HAc. The mixed samples were then homogenized on ice for 10 min. After centrifugation at 4 °C at 12,000 g for 30 min, the supernatants were filtered in Amicon Ultracel 10-kDa molecular weight cut-off filters (Millipore, Billerica, MA) by centrifugation, according to the manufacturer's instructions, to remove peptides larger than 10 kDa.

2.3. Peptide identification and characterization

Then the peptides were concentrated with a Savant Explorer SpeedVac (Thermo Fisher Scientific, Waltham, MA, USA), desalted, and finally lyophilized. The peptides derived from the different samples were labeled with 6-plex Tandem Mass Tag (TMT, Thermo Fisher Scientific, Waltham, MA, USA) reagents (Boersema et al., 2009).

Peptides Identification was performed on 1D Plus nano LC system (Eksigent, USA) coupled with Triple TOF 5600 system (Appied Biosystems, USA) according to the studies before (Li et al., 2018). The ionization Votalge was 2.3 kV and the tempreture was 120℃. A 15 cm × 75 μm i.d. fused silica capillary colume packed with 2 μm Jupiter C18-bonded particles (Phenomenex, Torrance, CA) was used for analysis of both normal ovarian epithelial samples and serous ovarian cancer samples. Peptides were subsequently eluted using the phase A (0.1% formic acid in water) and phase B (0.1% formic acid acetonitrile) with the following effective gradient profiles (min:B%): 0:3, 1:6, 60:23, 73:35, 75:80, 78:80, 78.1:5, 90:5, flow rate 300 nL/min). The TOF 5600 mass spectrometer was then operated in the data dependent acquisition mode acquiring high-resolution collision-induced dissociation scans and the normalized collision energy of 35 was used for collision-induced dissociation scans. MS spectra were recorded over an m/z range of 350 ~ 1250 in high resolution mode using 250 ms accumulation time per spectrum. The 20 most intense precursors were selected for fragmentation per cycle and the dynamic exclusion time was 9 s.

MS/MS spectra data were searched using PEAKS Studio (v7.0)software (Bioinformatics Solutions Inc., Waterloo, Canada), and the raw data were searched against the human Uniprot sequence database (20170718, 20,214 sequences), with MS1 tolerance of 20 ppm and MS2 tolerance of 0.1 Da. No enzyme and fixed modification were set in the search parameter. The false discovery rate (FDR) was fixed at 1% with a 2 unique peptide criterion. Students' t-test was applied to compare the peptide expression levels between two groups. FDR correction was then used for the adjustment of the p-value in the students' ttest. The total value of each group was used to calculate the fold change. And peptides with a fold change > 2 and FDR < 0.05 were considered as the differentially expressed peptides.

The mass difference of the TMT labels and their signal intensity in the secondary mass spectrometry was used to compare the quantitative information of peptides in different samples. The mass charge ratio of peptide fragment in the secondary mass spectrometry reflected the sequence information of peptides. In the LC/MS results, N1, N2 and N3 indicate the normal ovarian epithelial tissues, while T1, T2 and T3 indicate the serous ovarian cancer tissues.

2.4. Bioinformatics and bioactive peptide screening

The precursors of the differentially expressed peptide were mapped to Gene Ontology (GO) terms and Kyoto Encyclopedia of Genes and Genomes (KEGG) pathways using the Databases for Annotation, Visualization and Integrated Discovery (DAVID) website.

In recent years, a variety of websites had been developed for the prediction of specific functional peptides. In this study, we used the web server for designing peptide-based vaccine adjuvants, VaxinPAD (http://crdd.osdd.net/raghava/vaxinpad/team.php), which was developed by the research group of Dr. Gajendra P. S. Raghava (Bhalla et al., 2017); this group has been participating in the discovery of bioactive peptides, functional lncRNAs, and DNAs for many years. In addition, the possible antibacterial peptides were analyzed using the website developed by Dr. Susan Idicula-Thomas (http://www.campsign.bicnirrh.res.in/) (Waghu et al., 2016).

2.5. Cell culture and treatment

SKOV3 and OVCAR3 cells were purchased from the Cell bank of the Chinese Academy of Sciences. And both cells were culture in RPMI-1640 supplemented with 10% FBS and 1% Penicillin-Streptomycin mixture (100*). The peptides (> 95% purity) were synthesized by Shanghai Science Peptide Biological Technology Co.,ltd. and dissolved in the mixture of DMSO and mill Q (V:V = 1:4, used as the vehicle control) with a final concentration of 20 mM and preserved in -40℃ until use.

2.6. CCK8 assay

For cell proliferation assay, cells suspended in fresh medium supplemented with 100 μM P1DS or P1DP or vehicle were seeded at a density of 1000 cells per well in 96-well plates. Cell culture medium was changed into fresh media containing 10% (v/v) CCK8 reagent at indicated time point. Two hours after CCK8 reagent was added, the absorbance of each well was measured on a microplate reader at the wavelength of 450 nm. For the cell proliferation analysis at 48 h or 72 h, cell culture medium supplemented with 100 μM P1DS or P1DP or vesicle was changed every 24 h.

2.7. Transwell assay

For cell migration and invasion assay, polycarbonate cell culture inserts with pore size of 8.0 μm (Corning, NY, USA) were placed in 24-well plates. 5×10^4 cells in 200 μl serum-free medium containing vehicle, 100 μM of P1DP or P1DS were seeded into the upper chambers with or without Matrigel (BD Bioscience, Bedford, USA) for cell invasion and migration, respectively. And 700 μl fresh medium with 15% FBS was added to the lower chamber. For invasion assay, both OVCAR3 and SKOV3 cells were cultured for 48 h before analysis. And for migration assay, OVCAR3 cells were cultured for 36 h and SKOV3 cells were cultured for 24 h before analysis. Then the invaded/migrated cells on the bottom surface of the chamber were fixed in 4% paraformaldehyde for 1 h, stained with 0.5% crystal violet for 30 min and washed twice with PBS. After the cells in the upper chamber were eliminated using cotton swabs, three random selected fields per chamber were photographed under an EVOS XL Core digital microscope (Thermo Fisher Scientific, Waltham, USA). Finally, the crystal violet stained cells in the lower chamber were lysed in 200 μl lysis buffer (Invitrogen, Carlsbad, USA) and the absorbance (OD value) was measured at the wavelength of 575 nm in a microplate reader (BioTek Synergy H4).

2.8. Statistical analysis

Statistical analysis was performed using the two-tailed Student's *t*-test. The FDR-adjusted p-value (or q-value) was also calculated. $q < 0.05$ and fold changes ≥ 2 were considered statistically significant.

3. Results

3.1. Peptide profiling of serous ovarian cancer tissue and normal ovarian epithelial tissue from patients with benign ovarian tumors

A total of 3992 peptides from 1805 precursor proteins were identified in both the serous ovarian cancer tissue samples (3920 ± 36) and the normal ovarian epithelial tissue samples (3805 ± 76) **(**Fig. 1**A)**. The identified peptides were highly consistent across samples in both the ovarian cancer group (coefficient of variation = 2%) and the normal ovarian epithelial group (Coefficient of Variation = 0.93%). Principal Component Analysis (PCA) showed complete separation of the peptide profiles between the serous ovarian cancer tissues and the normal ovarian epithelial tissues (Fig. 1**B**). Heat map and volcano plot analysis identified 634 differentially expressed peptides (Fold change ≥ 2 and $q < 0.05$); 126 peptides from 108 precursor proteins were highly abundant in the normal epithelial ovarian tissues, and 508 peptides from 372 precursor proteins were enriched primarily in the serous ovarian cancer tissues (Fig. 1**C and D** and **Supplementary** Table 1). The isoelectric point (PI) and molecular weight (MW) of the differentially expressed peptides were consistently related to the proteolytic activity in the tissues. We found a PI between 5 and 9 for 35.8% of the upregulated peptides and 27.0% of the downregulated peptides, while we found a PI of > 11 or ≤ 4 for 27.6% of the upregulated peptides and 37.3% of the downregulated peptides. The MW of 74.0% of the upregulated peptides and 30.1% of the downregulated peptides was between 900 ~ 1500 Da, while the MW of 21.7% of the upregulated peptides and 64.3% of the downregulated peptides was > 1700 Da or < 900 Da (Fig. 1**E and F**). These results suggest both PI and MW differences between the upregulated and downregulated peptides in the serous ovarian cancer tissues.

3.2. Cleavage site analysis of the differentially expressed peptides

Peptidomics profiling is informative for the identification of the protein degradation activity in various types of cancer (Xu et al., 2015; Villanueva et al., 2006). To investigate differences in the degradomic profiles of cancerous and normal ovarian epithelial tissues, the cleavage sites of the differentially expressed peptides were analyzed. The results showed that the most frequently observed amino acids at the P1 position in the upregulated peptides of serous ovarian cancer tissues were P (Pro, 23.2%), L (Leu, 21.3%) and V (Val, 18.3%); compared with L (Leu, 27.8%), G (Gly, 19.0%) and V (Val, 18.3%) in the downregulated peptides (Fig. 2**A**). The most frequently observed amino acids at the P1' position in the upregulated peptides of serous ovarian cancer tissues were K (Lys, 27.8%), S (Ser, 17.5%) and T (Thr, 16.5%); compared with K (Lys, 20.6%), V (Val, 18.3%) and G (Gly, 18.3%) in the normal ovarian epithelial tissues. Furthermore, we also noticed that W (Trp) at the P1 position was only detected in the downregulated peptides of the serous ovarian cancer tissues **(**Fig. 2**B)**. The peptide bonds that were most frequently disrupted in the upregulated peptides of serous ovarian cancer tissues were L.K (2.4%), S.K (2.2%), P.K (2.2%) and E.K (2.2%) in the N terminal of the identified peptide, and P.S (2.2%), P.A (2.0%), P.V (1.6%) and L.L (1.6%) in the C-terminal of the identified peptide. The peptide bonds that were most frequently disrupted in the downregulated peptides of the ovarian cancer tissue were A.K (2.4%), I.K (2.4%), L.L (2.4%) and P.L (2.4%) in P1; and G.P (3.2%), L.K (3.2%), L.S (3.2%), P.G (3.2%), V.T (3.2%) and V.V (3.2%) in C-terminal of the identified peptide.

3.3. GO and pathway analysis of the precursor proteinss of the differentially expressed peptide

Most peptides function as part of their precursors or as inactivators of their precursors (Wang et al., 2016; Arpel et al., 2014; Soragni et al., 2016). To further investigate the potential function of the differentially expressed peptides, GO and pathway analyses of the precursor proteins of the differentially expressed peptides were performed. Our results showed that the top three subcellular localization sites of the precursors were the endoplasmic reticulum lumen, neuromuscular junction and membrane. The GO terms defining the top three biological pathways involved were the collagen catabolic process, extracellular matrix organization and cerebral cortex development. The GO terms defining the top three functional categorizations were ATP binding, extracellular matrix structural constituent and actin binding. The top three differentially regulated pathways were the focal adhesion, protein digestion and absorption and ECM-receptor interaction pathways **(**Fig. 3**)**, a triad that is highly consistent with the characterization of ovarian cancer.

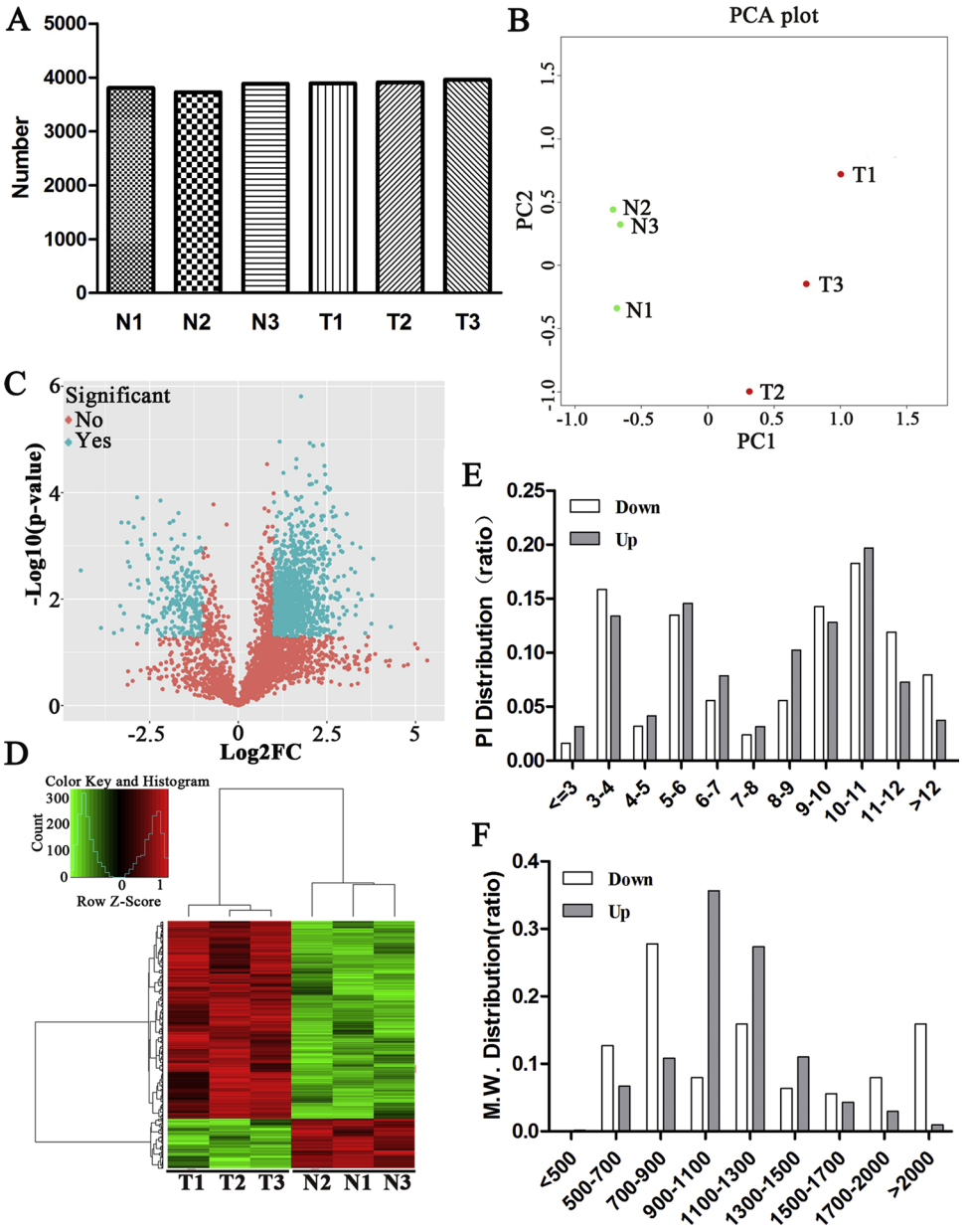

Fig. 1. Characteristics of peptides identified by Liquid Chromatography/Mass Spectrometry (LC/MS). (A) The number of identified peptides in each sample (N1, N2 and N3 indicate the normal ovarian epithelial tissues, while T1, T2 and T3 indicate the epithelial ovarian cancer tissues). (B) PCA analysis of the peptides identified in each tissue. (C) Volcano plot analysis of the peptides identified from the ovarian cancer tissues and the normal ovarian epithelial tissues (The blue dots indicate the differentially expressed peptides with fold change ≥2 and p-value < 0.05, while the red dots indicate the peptides whose expression was not significantly changed.). (D) Heat map of the differentially expressed peptides between the ovarian cancer tissues and the normal ovarian epithelial tissues with fold change ≥2 and q-value < 0.05) (The red lines indicate the peptides downregulated in the serous ovarian cancer tissues, and the green lines indicate the peptides upregulated peptides in the serous ovarian cancer tissues.). (E) Analysis of the isoelectric point (PI) distribution ratio in the upregulated and downregulated peptides. (F) Analysis of the molecular weight (MW) distribution ratio in the upregulated and downregulated.

3.4. Bioinformatic prediction of bioactive peptides

To find whether there are bioactive peptides in the differentially expressed peptides, we compared the sequences of the 634 differentially expressed peptides (**Supplementary** Table 1) with a positive dataset consisting of the sequences of both the 45 major antimicrobial peptide (AMP) families (Waghu et al., 2016) and the 305 experimentally validated, patented immunomodulatory peptide sequences from the peptide-based vaccine adjuvant design web server and with a negative dataset consisting of 385 peptides found endogenously in human plasma (http://crdd.osdd.

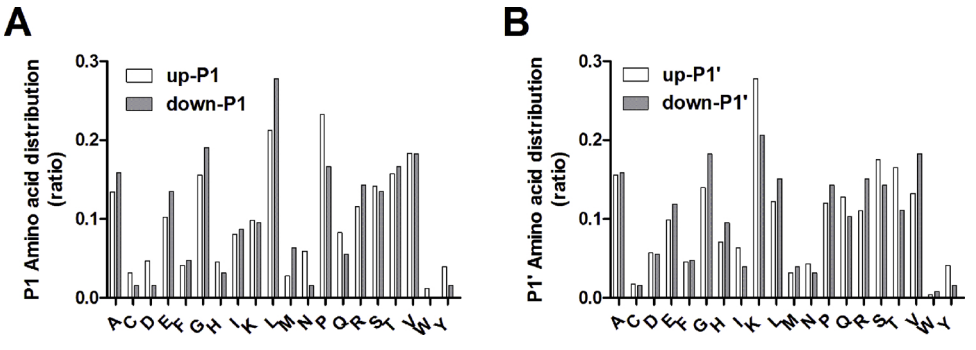

Fig. 2. Cleavage site specificity analysis of the differentially expressed peptides. Following previously established naming conventions, the C-terminal amino acid of the succeeding peptide was named as P1_up and the C-terminal amino acid of the identified peptide are named as P1_Down, and the N-terminal amino acid of the preceding peptide was named as P1'_up and the N-terminal amino acid of the identified peptide was named as P1'_down position. (A) The ratios of the P1_up and P1_down amino acids in the differentially expressed peptides. (B) The ratios of the P1'_up and P1'_down amino acids in the differentially expressed peptides.

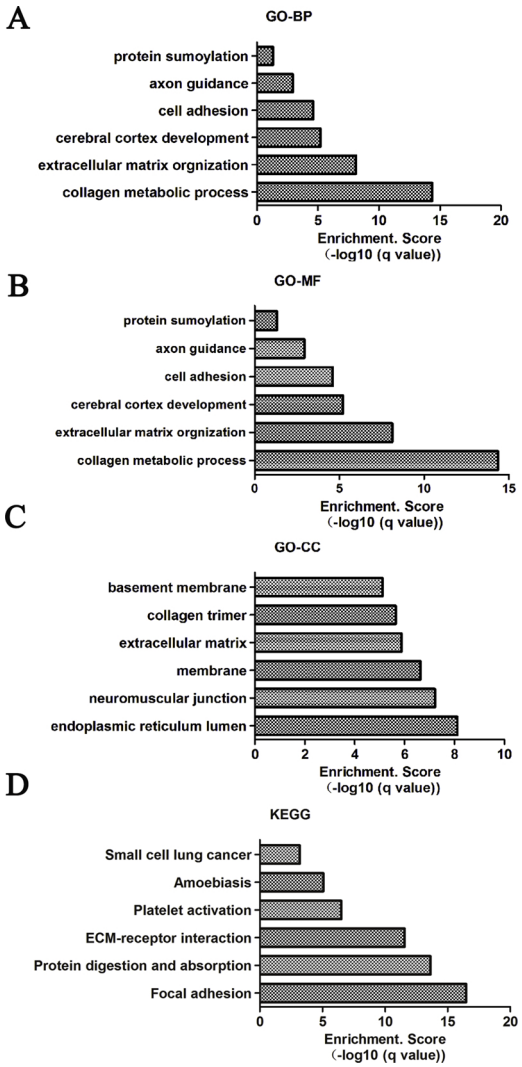

Fig. 3. GO and pathway analysis of the precursor proteins of the differentially expressed peptides. DAVID was used for the GO and pathway analysis of the precursor proteins of the differentially expressed peptides. (A) The top 6 biological processes, (B) the top 6 functional categories, (C) the top 6 subcellular localization sites, and (D) the top 6 KEGG pathways of the precursor proteins of the differentially expressed peptides.

net/raghava/vaxinpad/multi_submitfreq.php?ran = 42,560). We found that 11.1% (14/126) of the downregulated peptides and 9.45% (48/508) of the upregulated peptides were potential immune-regulated peptides (Table 1). All of the 634 peptides belong to the aurein AMP family, 7.2% (9/126) of the downregulated peptides and 3.74% (19/508) of the upregulated peptides possessed a sequence similar to aurein AMP family (http://www.campsign.bicnirrh.res.in/blastDB/) (Table 2). These results indicate that a proportion of the potential immune-regulated and AMP-like peptides that was enriched in the normal ovarian epithelial tissues were reduced in the serous ovarian cancer tissues. However, a proportion of peptides were also found to be significantly upregulated in the serous ovarian cancer tissues.

3.5. Are the peptide precursors unstable?

Our peptidomic analysis indicated that more than 80% of the differentially expressed peptides were upregulated in the serous ovarian cancer tissues. However, in comparing the precursor proteins of our differentially expressed peptides with the previously reported 600 proteins that have the highest turnover rate in HeLa cells (Boisvert et al., 2012), we found that only 5 of the precursor proteins overlapped (**Supplementary** Table 2). Among the 78 precursor proteins identified in our study that had ≥2 differentially expressed peptides, 37 were precursors with both upregulated and downregulated peptides (**Supplementary** Table 3). Therefore, we postulate that the differentially expressed peptides are not just the degradation products of their corresponding precursor proteins.

3.6. Peptide P1DS significantly inhibit the invasion and migration of ovarian cancer cells

To further analyze the differentially expressed peptide function in ovarian cancer cells, we randomly selected 2 down-regulated peptides (Peptide 1 derived from PAPD7, abbreviated as P1DP; peptide 1 derived from S38AA protein, abbreviated as P1DS) in ovarian cancer tissues Table 3, and analyzed the cell proliferation, invasion and migration of SKOV3 and OVCAR3 ovarian cancer cells after treatment with P1DS or P1DP peptide. Interestingly, CCK8 assay indicated that none of the peptides affected the proliferation of ovarian cancer cells (Fig. 4**A**). However, P1DS significantly inhibited invasion and migration of OVCAR3 and SKOV3 ovarian cancer cells. While P1DP did not affect the cell invasion and migration significantly, although it is 21 fold higher in normal ovarian epithelium compared with ovarian cancer tissues (Fig. 4**B-E**).

4. Discussion

To date, the anticancer peptides on the market have generated an enormous economic value. These small peptides, which are designed by targeting oncogenes, mutated or inactivated tumor suppressors, the tumor microenvironment and the immune system of patients, have shown great anticancer potential (Wang et al., 2016; Arpel et al., 2014; Soragni et al., 2016; Catena et al., 2013). As small-molecule drugs, therapeutic peptides have greater specificity and lower toxicity, as well as a short half-life (Wu et al., 2014; Cai et al., 2013). Although their poor stability, easy to be degraded and difficult to pass through intestinal mucosa when taken orally restricted their clinical application, scientists have done a lot of basic work for the modification of peptides, further selection of the modified peptides with higher specificity and cell membrane penetration ability, or using targeted delivery system, such as the Nanoscale Drug Carriers (Wang et al., 2016; Penchala et al., 2015; Du et al., 2018). Thus, we believe that peptide drugs possess immense future potential.

In recent years, antitumor activity has been observed in an increasing number of endogenous peptides, such as the peptide released from therapy-sensitive cancer cells that can overcome therapeutic resistance, and the persistent peptide antigens that can be given exogenously as an anticancer vaccine (Hebbar et al.,2017; Nakagawa et al., 2017).

Our bodies are rich in therapeutic molecules. More anti-cancer or anti-infection mechanisms have been recognized or are being recognized. More importantly, researchers have recently observed an anticancer effect in nearby normal skin epithelial cells (Brown et al., 2017). The endogenous peptide, HBD2 which is enriched in the healthy controls and decreased in hypertension patients exerted hypotensive function effect in Monkeys significantly at 4× to 6× physiological concentration (Liu et al., 2013). The endogenous peptide apelin which is induced by muscle contraction can enhance muscle function in myofibers and enhancing the muscle regenerative capacity (Claire et al., 2018). And the pancreatic polypeptide which is secreted from endocrine pancreas can predict visceral and liver fat content (Sam et al., 2015). Interestingly, peptidome profiles can effectively distinguish different cancer types and cell lines, as well as body fluids (e.g., blood serum and uterine fluid) (Liu et al., 2016; Xu et al., 2015; Greening et al., 2013; Dai et al., 2017). However, only a few studies proceeded to determine the function of the differentially expressed peptides, with limited studies confirming the bioactivity of peptides found in human

Table 1
The differentially expressed peptides with potential immunoregulatory activity (Fold change > 2 and FDR < 0.05).

Sequence	Gene name	log2(FC)	p-value	q-value
RRQLRTRK	KI67	−2.1709	0.006666	0.044318
FKIFLKYL	SACS	−2.03473	0.004855	0.039717
HKTDPSAAVRKKKQRHGEAV	EP400	−1.94115	0.006185	0.042905
QKPAKPV	GRD2I	−1.72616	0.005908	0.042804
VVSVPAAV	EP400	−1.70644	0.001752	0.029845
QSAIKHNVKSLITGPSKLSRG	NCOR1	−1.51948	0.000615	0.02647
SAIVHSR	K1107	−1.4625	0.003128	0.03552
EVPIPTRFL	S4 A8	−1.42665	0.002845	0.035439
LASPAVPAPG	HJURP	−1.38844	0.00375	0.037584
KMVALKGI	KMT2D	−1.19358	0.001282	0.027847
VPPFRVPLPGMPIPLP	TCRG1	−1.19358	0.001282	0.027847
RRKMSKKLP	DPOLZ	−1.1745	0.007264	0.046322
EAILPKGSARV	EP400	−1.10363	0.000697	0.027005
AVEKLILKSGK	F178A	−1.04572	0.001093	0.027847
SASVLTVRRE	CO7A1	1.022141	0.003247	0.035609
KFPGSAALVGAVRKP	DIDO1	1.037149	0.006176	0.042905
KLKAIEYV	PRSR1	1.074173	0.008519	0.049372
MAKRVANLLR	NUP98	1.088152	0.006394	0.043713
KTVQIAKKPR	LIN54	1.14313	0.00216	0.031692
FVFKTRAC	DOC10	1.151662	0.006566	0.044197
RVLYIRYR	TPPC9	1.158	0.000234	0.022317
GLAKKYRDNRT	KC1 AL	1.166319	0.006653	0.044318
RFVRTAIPF	CYFP2	1.211393	0.00323	0.03552
GIVGHTVR	ADCYA	1.254836	0.007594	0.047276
TQKPAKPVPGP	GRD2I	1.286927	0.000806	0.027847
KTKVNVKSVKRNT	PHF3	1.317219	0.002188	0.031696
YGNRITVH	MXRA5	1.336	0.005931	0.042893
VPAHLSRKT	H1FOO	1.353594	0.002193	0.031696
AGTGSRKRV	CELR3	1.363687	0.003002	0.03552
KSLKCLA	ARMC4	1.364298	0.006625	0.044228
EVIITGCVKE	PAR14	1.389039	0.000111	0.01915
AISVQALNAK	FCGBP	1.421772	0.00609	0.042905
LPSVMAGVPARRG	WDR62	1.470833	0.006529	0.0441
QTCLKPITASKVEFAI	CORA1	1.499414	0.00132	0.027847
KGNSKKVVQ	RNF8	1.523171	0.00043	0.023979
VLKSYIGLG	CLCN6	1.532492	0.004881	0.039848
ERLKSVPADPAPPS	SSH1	1.580912	0.003432	0.036293
HSTAKVVL	SIRBL	1.588064	0.008765	0.049473
KLNSKRVSFKLPKD	CASC5	1.591353	0.006072	0.042905
SLKTAVISIG	SYNE2	1.602126	0.004507	0.038915
HGNVKV	MRF	1.655262	0.0038	0.037584
KVPSEVVP	NACAM	1.671408	0.005652	0.042094
VPVVRLAGS	GPR98	1.677775	0.006797	0.044848
RIGVFPSVL	FCSD2	1.748067	0.001442	0.027847
RLISKPRVGR	AHNK2	1.774569	0.00097	0.027847
KKGQVPGPARSE	ZN469	1.792561	0.001446	0.027847
AKALAKQCVV	DYH3	1.802944	0.008784	0.049473
KTMKVTGV	FA8	1.977208	0.008678	0.049464
ITAVGSFN	T22D1	1.993116	0.00191	0.030425
TVPVPPAAV	WNK2	2.007094	0.002323	0.032746
ASMKVKHVKKLPF	RHG32	2.013956	0.00588	0.04274
ESKKLIKAV	RPC6	2.203355	6.23E-05	0.017454
HPIRLGLAL	1433Z	2.285235	0.001752	0.029845
TKAMLKKP	BICC1	2.305922	0.001095	0.027847
QHRANAKSAKT	CEL	2.349768	0.001439	0.027847
RLKRQFSIFN	DYH5	2.373555	0.002207	0.031696
CRLRGRVALA	MED16	2.626302	0.000227	0.022317
RALTRGHGATR	PLXA3	2.821806	0.007769	0.04757
KVYVPALIFG	TOP2B	3.219851	0.000902	0.027847
TGKVGMLKNLK	FSTL4	3.808147	0.001753	0.029845
KLDLKVPK	AHNK2	#DIV/0!	0.000587	0.02647
NIYLPHVMLLAKIKMRIGHTVAK	CFA54	#DIV/0!	0.008476	0.049372

#DIV/0!: Not detected in the normal ovarian epithelial.

tissues, biofluids, animals, and plants (Penchala et al., 2015; Ledwidge et al., 2015; Marx et al., 2013; Thell et al., 2016; Liu et al., 2013). The bioinformatic analysis of the differentially expressed peptides in our study also supports the existing evidence in favor of bioactive endogenous peptides.

Most peptides are the proteolytic products of precursor proteins (Greening et al., 2013). Previous studies have demonstrated the elevated activity of extracellular proteases and matrix metallopeptidases that results in an increased abundance of peptides derived from extracellular precursor proteins (Kondakova et al., 2012). However, only 5

Table 2
The differentially expressed peptides with similar sequence of the aurein AMP family (Fold change > 2 and FDR < 0.05).

Sequence	Gene name	log2(FC)	p-value	q-value
QLPSVPVPAPASTPPPVPVLAPAPAPAPAPVAA	CDN1C	−2.1286	0.004303	0.038753
SPTPRIGWTVNDRPVTEGVSEQDGGSTLQRAAVSRE	HMCN2	−1.94115	0.006185	0.042905
VDFRSVLAKKGTSKTPVPEKVPPPKPATP	MYLK	−1.94115	0.006185	0.042905
PPAILPVAAPTPVVPSSAPAAVAK	YETS2	−1.73904	0.008826	0.049473
AALRVLGAAGAVGR	PRR36	−1.44584	0.00376	0.037584
QPSVKPAAAKPAPAKPVAAK	CO6A3	−1.29025	0.003205	0.03552
ECAEEGYCSQG	LRP4	−1.2393	0.003089	0.03552
VPGVGVPGAGIPVVPGAG	ELN	−1.19358	0.001282	0.027847
PPLVTAVVPPAGPLVLS	NTM2F	−1.17474	0.006103	0.042905
KGAAPAPPGKT	TCOF	1.03023	0.00413	0.038692
VVAPGPPVTTATSAPV	TB10B	1.032943	0.006191	0.042905
PSPLQPPAAPAPTST	TAOK2	1.216648	0.003157	0.03552
TTLLGGKEAQALGVPGGS	LENG9	1.387121	0.008492	0.049372
GFPAALPAGPAG	KMT2D	1.505767	0.008799	0.049473
KTVQKFWHKILPFV	ABCAD	1.508078	0.004946	0.03987
LPGPPGKKGQA	COFA1	1.618764	0.005464	0.041554
YGGDVLAGPGGGGG	ZNT5	1.685228	0.000413	0.023979
KTGGKARAKA	H2AX	1.769238	0.007176	0.045959
GGPAPAAAAAAAAV	DMBX1	1.8842	0.004655	0.039377
SLPALGAGAAAGSAAAAAA	VAX1	1.968214	0.000565	0.02647
PAAAAPASTGAPPGG	IRX2	2.022397	0.006599	0.044197
TPGKGATPAPPGKAG	TCOF	2.233497	0.002652	0.034926
HVKAFAHITGGGL	PUR2	2.451537	0.006289	0.043214
AGVPEGPGFCPQ	CO5A3	2.569981	0.002167	0.031692
HGALGSKPPAGGPSP	EP400	2.720865	0.004513	0.038915
PVVAAPPSLRVPRPPPL	EP400	#DIV/0!	0.003133	0.03552
GLEPPAAREPALSRAGS	CGAS	#DIV/0!	0.00153	0.028541

#DIV/0!: Not detected in the normal ovarian epithelial tissues. Here, we presented the intersection of the differentially expressed peptides having the similar sequence with the aurein AMP family using different scoring matrix (BLOSUM62, BLOSUM45, BLOSUM80, PAM30 and PAM70).

Table 3
The properties of the 2 randomly selected down-regulated peptides in ovarian cancer tissues.

Sequence	Gene name	log2(FC)	p-value	q-value
TAGNVLMH	S38AA	−9.810408696	0.000364	0.024242
RAAALSGGGGP	PAPD7	−21.71707077	0.002897	0.03569

peptide precursor proteins are overlapped with the top 600 proteins in HELA cells with the highest turnover rate. And both up-regulated and down-regulated peptides exist in the precursor proteins with ≥2 differentially expressed peptides, which indicate that the differentially expressed peptides are not just the degradation products of their precursor proteins.

Most ovarian cancer patients experienced peritoneal or omental metastasis. Focal adhesion and ECM-receptor interactions are important regulators of ovarian cancer metastasis (Annunziata and Kohn, 2013; Zhu et al., 1995). Rapid recycling of RNA and proteins is essential for the rapid proliferation of cancer cells. Our KEGG pathway analysis indicated that the differentially expressed peptide precursors are primarily involved in the focal adhesion, protein digestion and absorption and ECM-receptor interaction pathways, a triad that is highly consistent with the characterization of ovarian cancer. Indeed, most bioactive peptides function as part of their precursors or as in-activators of their precursors (Wang et al., 2016; Soragni et al., 2016). These attributes indicate that the differentially expressed peptides found in our study may be involved in the progression of ovarian cancer. In addition, immunohistochemical analysis of anti-type I collagen antibodies specific for newly synthesized and cross-linked mature type I collagen suggested that collagen metabolism is very prevalent in malignant ovarian tumors (Multhaupt et al., 2016). Extracellular matrix organization has also been proposed to be important for cancer metastasis (Gilkes et al., 2014; Multhaupt et al., 2016). Our results are the first to confirm that the peptides derived from precursors which are important in collagen metabolism and extracellular matrix organization are also differentially regulated in serous ovarian cancer tissues. Interestingly, we noted that the neuromuscular junction cellular component and the cerebral cortex development biological process are also differentially regulated in ovarian cancer. Indeed, we found that molecules that are crucial for neuromuscular junction development are also important for cancer progression; for example, integrin α3 and agrin (Ross et al., 2017; Xiong and Mei, 2017; Varzavand et al., 2016).

Besides, we found that P1DS can significantly inhibit invasion and migration of ovarian cancer cells, but did not affect the proliferation of ovarian cancer cells. These results indicated that bioactive peptides exist in vivo involved in the progression of ovarian cancer.

However, the concentration of the peptides used is a little high and the mechanism of the peptide function in ovarian cancer progression still needs to be further investigated.

Funding

This study was supported by the National Natural Science Foundation of China (Grant numbers: 81602285, 81872126, 81572556, Nanjing Medical Science and technique Development Foundation (Grant numbers: JQX17009 & ZDX16015), Nanjing Technological Development Program (Grant number: 201605053), Jiangsu Provincial Medical Talent (Xuemei Jia) and Nanjing Medical Youth Talent(Grant number: qnrc259).

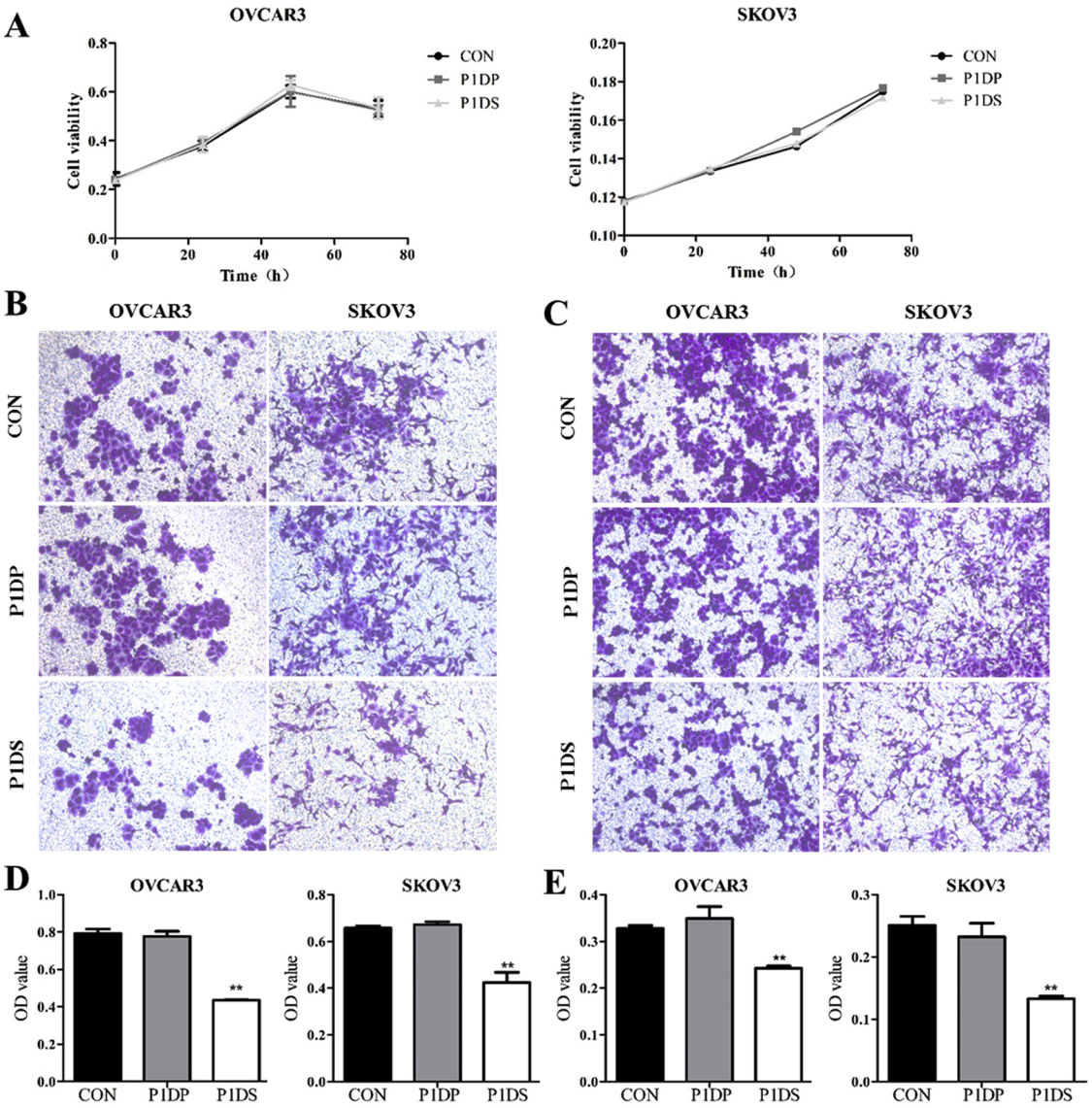

Fig. 4. P1DS peptide significantly inhibited the invasion and migration of ovarian cancer cells. (A) The cell proliferation of OVCAR3 and SKOV3 ovarian cancer cells were analyzed 0 h, 24 h, 48 h and 72 h after P1DS, P1DP or vesicle treatment. (B) The representative image of the invaded cells and migrated cells of OVCAR3 and SKOV3 cells. (C) The representative image of the migrated cells of OVCAR3 and SKOV3 cells. (D) The protein concentration of the invaded cells of OVCAR3 and SKOV3 cells was analyzed using a microplate reader at a wavelength of 575 nm. (E) The protein concentration of the migrated cells of OVCAR3 and SKOV3 cells was analyzed using a microplate reader at a wavelength of 575 nm. $^{**}p < 0.01$.

Conflicts of interest

The authors have no conflicts of interest to declare.

Acknowledgements

We thank American Journal Experts who providing language help.

Appendix A. Supplementary data

Supplementary material related to this article can be found, in the online version, at doi:https://doi.org/10.1016/j.biocel.2018.12.004.

References

Annunziata, C.M., Kohn, E.C., 2013. Novel facts about FAK: new connections to drug resistance? J. Natl. Cancer Inst. 105, 1430–1431. https://doi.org/10.1093/jnci/djt255.

Arpel, A., Sawma, P., Spenlé, C., Fritz, J., Meyer, L., Garnier, N., Velázquez-Quesada, I., Hussenet, T., Aci-Sèche, S., Baumlin, N., Genest, M., Brasse, D., Hubert, P., Crémel, G., Orend, G., Laquerrière, P., Bagnard, D., 2014. Transmembrane domain targeting peptide antagonizing ErbB2/Neu inhibits breast tumor growth and metastasis. Cell Rep. 8, 1714–1721. https://doi.org/10.1016/j.celrep.2014.07.044.

Bhalla, S., Verma, R., Kaur, H., Kumar, R., Usmani, S.S., Sharma, S., Raghava, G.P.S., 2017. CancerPDF: a repository of cancer-associated peptidome found in human biofluids. Sci. Rep. 7, 1511. https://doi.org/10.1038/s41598-017-01633-3.

Boersema, P.J., Raijmakers, R., Lemeer, S., Mohammed, S., Heck, A.J.R., 2009. Multiplex peptide stable isotope dimethyl labeling for quantitative proteomics. Nat. Protoc. 4, 484–494. https://doi.org/10.1038/nprot.2009.21.

Boisvert, F.-M., Ahmad, Y., Gierliński, M., Charrière, F., Lamont, D., Scott, M., Barton, G., Lamond, A.I., 2012. A quantitative spatial proteomics analysis of proteome turnover in human cells. Mol. Cell Proteomics 11https://doi.org/10.1074/mcp.M111.011429.M111.011429.

Brown, S., Pineda, C.M., Xin, T., Boucher, J., Suozzi, K.C., Park, S., Matte-Martone, C., Gonzalez, D.G., Rytlewski, J., Beronja, S., Greco, V., 2017. Correction of aberrant growth preserves tissue homeostasis. Nature 548, 334–337. https://doi.org/10.1038/nature23304.

Cai, Y., Wei, L., Ma, L., Huang, X., Tao, A., Liu, Z., Yuan, W., 2013. Long-acting preparations of exenatide. Drug Des. Devel. Ther. 7, 963–970. https://doi.org/10.2147/DDDT.S46970.

Catena, R., Bhattacharya, N., El Rayes, T., Wang, S., Choi, H., Gao, D., Ryu, S., Joshi, N., Bielenberg, D., Lee, S.B., Haukaas, S.A., Gravdal, K., Halvorsen, O.J., Akslen, L.A., Watnick, R.S., Mittal, V., 2013. Bone marrow-derived Gr1 + cells can generate a

metastasis-resistant microenvironment via induced secretion of thrombospondin-1. Cancer Discov. 3, 578–589. https://doi.org/10.1158/2159-8290.CD-12-0476.
Claire, V., laura, L., Aurelie, B., Simon, D., Jean-Philippe, P., Sophie, Le.G., Alizée, D., Nancy, G., Ophelie, P., Sonia, K., Umji, L., Mylène, C., Karima, C., Etienne, M., Anne, B., Vincent, M., Mathieu, V., Allan, F.P., Angèle, C., Fabien, P., Sophie, G., Matteo, C., Odile, B.S., Marco, P., Jerome, N.F., Bruno, V., Philippe, V., Cedric, D., 2018. The exerkine apelin reverses age-associated sarcopenia. Nat. Med. 24 (9), 1360–1371. https://doi.org/10.1038/s41591-018-0131-6.
Dai, X., Song, X., Rui, C., Meng, L., Xue, X., Ding, H., Shen, R., Li, J., Li, J., Lu, Y., Long, W., 2017. Peptidome analysis of human serum from normal and preeclamptic pregnancies. J. Cell. Biochem. 118, 4341–4348. https://doi.org/10.1002/jcb.26087.
Du, C., Qi, Y., Zhang, Y., Wang, Y., Zhao, X., Min, H., Han, X., Lang, J., Qin, H., Shi, Q., Zhang, Z., Tian, X., Anderson, GJ., Zhao, Y., Nie, G., Yang, Y., 2018. Epidermal Growth Factor Receptor-Targeting Peptide Nanoparticles Simultaneously Deliver Gemcitabine and Olaparib To Treat Pancreatic Cancer with Breast Cancer 2 (BRCA2) Mutation. ACS. Nano. [Epub ahead of print] https://doi: 10.1021/acsnano.8b01573.
Frøssing, S., Nylander, M., Chabanova, E., Frystyk, J., Holst, J.J., Kistorp, C., Skouby, S.O., Faber, J., 2017. Effect of liraglutide on ectopic fat in polycystic ovary syndrome: a randomized clinical trial, in: diabetes. Obe. Metab. 215–218. https://doi.org/10.1111/dom.13053.
Gaborit, B., Darmon, P., Ancel, P., Dutour, A., 2016. Liraglutide for patients with non-alcoholic steatohepatitis. Lancet 387, 2378–2379. https://doi.org/10.1016/S0140-6736(16)30734-6.
Gilkes, D.M., Semenza, G.L., Wirtz, D., 2014. Hypoxia and the extracellular matrix: drivers of tumour metastasis. Nat. Rev. Cancer 14, 430–439. https://doi.org/10.1038/nrc3726.
Greening, D.W., Kapp, E.A., Ji, H., Speed, T.P., Simpson, R.J., 2013. Colon tumour secretopeptidome: insights into endogenous proteolytic cleavage events in the colon tumour microenvironment. Biochim. Biophys. Acta - Proteins Proteomics 1834, 2396–2407. https://doi.org/10.1016/j.bbapap.2013.05.006.
Hebbar, N., Burikhanov, R., Shukla, N., Qiu, S., Zhao, Y., Elenitoba-Johnson, K.S.J., Rangnekar, V.M., 2017. A naturally generated decoy of the prostate apoptosis Response-4 protein overcomes therapy resistance in tumors. Cancer Res. 77 (15), 4039–4050. https://doi.org/10.1158/0008-5472.CAN-16-1970.
Kondakova, I.V., Spirina, L.V., Shashova, E.E., Koval', V.D., Kolomiets, L.A., Chernysheva, A.L., Slonimskaia, E.M., 2012. Proteasome activity in tumors of female reproductive system. Bioorg. Khim. 38, 106–110.
Lauressergues, D., Couzigou, J.M., San Clemente, H., Martinez, Y., Dunand, C., Bécard, G., Combier, J.P., 2015. Primary transcripts of microRNAs encode regulatory peptides. Nature 520, 90–93. https://doi.org/10.1038/nature14346.
Ledwidge, M.T., O'Connell, E., Gallagher, J., Tilson, L., James, S., Voon, V., Bermingham, M., Tallon, E., Watson, C., O'Hanlon, R., Barry, M., McDonald, K., 2015. Cost-effectiveness of natriuretic peptide-based screening and collaborative care: a report from the STOP-HF (St Vincent's Screening to prevent Heart Failure) study. Eur. J. Heart Fail. 17, 672–679. https://doi.org/10.1002/ejhf.286.
Li, J., Chen, L., Li, Q., Cao, J., Gao, Y., Li, J., 2018. Comparative peptidomic profile between human hypertrophic scar tissue and matched normal skin for identification of endogenous peptides involved in scar pathology. J. Cell. Physiol. 233, 5962–5971. https://doi.org/10.1002/jcp.26407.
Liu, R., Zhang, Z., Liu, H., Hou, P., Lang, J., Wang, S., Yan, H., Li, P., Huang, Z., Wu, H., Rong, M., Huang, J., Wang, H., Lv, L., Qiu, M., Ding, J., Lai, R., 2013. Human β-defensin 2 is a novel opener of Ca2 + -activated potassium channels and induces vasodilation and hypotension in monkeys. Hypertension 62, 415–425. https://doi.org/10.1161/HYPERTENSIONAHA.111.01076.
Liu, F., Zhao, C., Liu, L., Ding, H., Huo, R., Shi, Z., 2016. Peptidome profiling of umbilical cord plasma associated with gestational diabetes-induced fetal macrosomia. J. Proteomics 139, 38–44. https://doi.org/10.1016/j.jprot.2016.03.001.
Mann, J.F.E., Ørsted, D.D., Brown-Frandsen, K., Marso, S.P., Poulter, N.R., Rasmussen, S., Tornøe, K., Zinman, B., Buse, J.B., 2017. Liraglutide and renal outcomes in type 2 diabetes. New Engl. J. Med. 377, 839–848. https://doi.org/10.1056/NEJMoa1616011.
Marx, N., Silbernagel, G., Brandenburg, V., Burgmaier, M., Kleber, M.E., Grammer, T.B., Winkelmann, B.R., Boehm, B.O., Marz, W., 2013. C-Peptide levels are associated with mortality and cardiovascular mortality in patients undergoing angiography: the LURIC study. Diabetes Care 36, 708–714. https://doi.org/10.2337/dc12-1211.
Matsumoto, A., Pasut, A., Matsumoto, M., Yamashita, R., Fung, J., Monteleone, E., Saghatelian, A., Nakayama, K.I., Clohessy, J.G., Pandolfi, P.P., 2017. MTORC1 and muscle regeneration are regulated by the LINC00961-encoded SPAR polypeptide. Nature 541, 228–232. https://doi.org/10.1038/nature21034.
Multhaupt, H.A.B., Leitinger, B., Gullberg, D., Couchman, J.R., 2016. Extracellular matrix component signaling in cancer. Adv. Drug Deliv. Rev. 7, 963–970. https://doi.org/10.1016/j.addr.2015.10.013.
Nakagawa, H., Mizukoshi, E., Kobayashi, E., Tamai, T., Hamana, H., Ozawa, T., Kishi, H., Kitahara, M., Yamashita, T., Arai, K., Terashima, T., Iida, N., Fushimi, K., Muraguchi, A., Kaneko, S., 2017. Association between high-avidity T-Cell receptors, induced by α-fetoprotein – derived peptides, and anti-tumor effects in patients with hepatocellular carcinoma. Gastroenterology. 152, 1395–1406. https://doi.org/10.1053/j.gastro.2017.02.001. e10.
Penchala, S.C., Miller, M.R., Pal, A., Dong, J., Madadi, N.R., Xie, J., Joo, H., Tsai, J., Batoon, P., Samoshin, V., Franz, A., Cox, T., Miles, J., Chan, W.K., Park, M.S., Alhamadsheh, M.M., 2015. A biomimetic approach for enhancing the in vivo half-life of peptides. Nat. Chem. Biol. 11, 793–798. https://doi.org/10.1038/nchembio.1907.
Ross, J.A., Webster, R.G., Lechertier, T., Reynolds, L.E., Turmaine, M., Bencze, M., Jamshidi, Y., Cetin, H., Muntoni, F., Beeson, D., Hodilvala-Dilke, K., Conti, F.J., 2017. Multiple roles of integrin-α3 at the neuromuscular junction. J. Cell. Sci. 130, 1772–1784. https://doi.org/10.1242/jcs.201103.
Sam, A.H., Sleeth, M.L., Thomas, E.L., Ismail, N.A., Mat, Daud.N., Chambers, E., Shojaee-Moradie, F., Umpleby, M., Goldstone, A.P., Le Roux, C.W., Bech, P., Busbridge, M., Laurie, R., Cuthbertson, D.J., Buckley, A., Ghatei, M.A., Bloom, S.R., Frost, G.S., Bell, J.D., Murphy, K.G., 2015. Circulating pancreatic polypeptide concentrations predict visceral and liver fat content. J. Clin. Endocrinol. Metab. 100 (3), 1048–1052. https://doi.org/10.1210/jc.2014-3450.
Selivanova, G., Iotsova, V., Okan, I., Fritsche, M., Ström, M., Groner, B., Grafström, R.C., Wiman, K.G., 1997. Restoration of the growth suppression function of mutant p53 by a synthetic peptide derived from the p53 C-terminal domain. Nat. Med. 3, 632–638. https://doi.org/10.1038/nm0697-632.
Soragni, A., Janzen, D.M., Johnson, L.M., Lindgren, A.G., Thai-Quynh Nguyen, A., Tiourin, E., Soriaga, A.B., Lu, J., Jiang, L., Faull, K.F., Pellegrini, M., Memarzadeh, S., Eisenberg, D.S., 2016. A designed inhibitor of p53 aggregation rescues p53 tumor suppression in ovarian carcinomas. Cancer Cell 29, 90–103. https://doi.org/10.1016/j.ccell.2015.12.002.
Szafron, L.M., Balcerak, A., Grzybowska, E.A., Pienkowska-Grela, B., Felisiak-Golabek, A., Podgorska, A., Kulesza, M., Nowak, N., Pomorski, P., Wysocki, J., Rubel, T., Dansonka-Mieszkowska, A., Konopka, B., Lukasik, M., Kupryjanczyk, J., 2015. The novel gene CRNDE encodes a nuclear peptide (CRNDEP) which is overexpressed in highly proliferating tissues. PLoS One 10, e0127475. https://doi.org/10.1371/journal.pone.0127475.
Thell, K., Hellinger, R., Sahin, E., Michenthaler, P., Gold-Binder, M., Haider, T., Kuttke, M., Liutkevičiūtė, Z., Göransson, U., Gründemann, C., Schabbauer, G., Gruber, C.W., 2016. Oral activity of a nature-derived cyclic peptide for the treatment of multiple sclerosis. Proc. Natl. Acad. Sci. 113, 3960–3965. https://doi.org/10.1073/pnas.1519960113.
Varzavand, A., Hacker, W., Ma, D., Gibson-Corley, K., Hawayek, M., Tayh, O.J., Brown, J.A., Henry, M.D., Stipp, C.S., 2016. α3β1 integrin suppresses prostate cancer metastasis via regulation of the Hippo pathway. Cancer Res. 76, 6577–6587. https://doi.org/10.1158/0008-5472.CAN-16-1483.
Villanueva, J., Shaffer, D.R., Philip, J., Chaparro, C.A., Erdjument-Bromage, H., Olshen, A.B., Fleisher, M., Lilja, H., Brogi, E., Boyd, J., Sanchez-Carbayo, M., Holland, E.C., Cordon-Cardo, C., Scher, H.I., Tempst, P., 2006. Differential exoprotease activities confer tumor-specific serum peptidome patterns. J. Clin. Invest. 116, 271–284. https://doi.org/10.1172/JCI26022.
Waghu, F.H., Barai, R.S., Idicula-Thomas, S., 2016. Leveraging family-specific signatures for AMP discovery and high-throughput annotation. Sci. Rep. 6, 24684. https://doi.org/10.1038/srep24684.
Wang, S., Blois, A., El Rayes, T., Liu, J.F., Hirsch, M.S., Gravdal, K., Palakurthi, S., Bielenberg, D.R., Akslen, L.A., Drapkin, R., Mittal, V., Watnick, R.S., 2016. Development of a prosaposin-derived therapeutic cyclic peptide that targets ovarian cancer via the tumor microenvironment. Sci. Transl. Med. 8, 329ra34. https://doi.org/10.1126/scitranslmed.aad5653.
Wu, D., Gao, Y., Qi, Y., Chen, L., Ma, Y., Li, Y., 2014. Peptide-based cancer therapy: opportunity and challenge. Cancer Lett. 351 (1), 13–22. https://doi.org/10.1016/j.canlet.2014.05.002.
Xiong, W.C., Mei, L., 2017. Agrin to YAP in Cancer and neuromuscular junctions. Trends. Cancer 3 (4), 247–248. https://doi.org/10.1016/j.trecan.2017.03.005.
Xu, Z., Wu, C., Xie, F., Slysz, G.W., Tolic, N., Monroe, M.E., Petyuk, V.A., Payne, S.H., Fujimoto, G.M., Moore, R.J., Fillmore, T.L., Schepmoes, A.A., Levine, D.A., Townsend, R.R., Davies, S.R., Li, S., Ellis, M., Boja, E., Rivers, R., Rodriguez, H., Rodland, K.D., Liu, T., Smith, R.D., 2015. Comprehensive quantitative analysis of ovarian and breast cancer tumor peptidomes. J. Proteome Res. 14, 422–433. https://doi.org/10.1021/pr500840w.
Xue, Y., Xu, P., Xu, S., Xue, K., Xu, L., Chen, J., Xu, J., Shi, X., Li, Q., Gu, L., 2018. Peptidomic analysis of endometrial tissue from patients with ovarian endometriosis. Cell. Physiol. Biochem. 47, 107–118. https://doi.org/10.1159/000489753.
Zhou, J., Zhao, M., Tang, Y., Wang, J., Wei, C., Gu, F., Lei, T., Chen, Z., Qin, Y., 2016. The milk-derived fusion peptide, ACFP, suppresses the growth of primary human ovarian cancer cells by regulating apoptotic gene expression and signaling pathways. BMC Cancer 16, 246. https://doi.org/10.1186/s12885-016-2281-6.
Zhu, G.G., Risteli, L., Mäkinen, M., Risteli, J., Kauppila, A., Stenbäck, F., 1995. Immunohistochemical study of type I collagen and type I pN-collagen in benign and malignant ovarian neoplasms. Cancer. 75, 1010–1017. https://doi.org/10.1002/1097-0142(19950215)75:4&1010::AID-CNCR2820750417&3.0.CO;2-O.